UTM UNIVERSITI TEKNOLOGI MALAYSIA

IJBES

International Journal of Built Environment and Sustainability
Published by Penerbit UTM Press, Universiti Teknologi Malaysia
IJBES 13(3)/2026, 283-304

Impact of Shading Devices for Faculty Office Buildings in Tropical Regions—A Case Study in Malaysia

Jian Peng
Faculty of Built Environment and Surveying, Universiti Teknologi Malaysia, 81310 UTM Johor Bahru, Johor, Malaysia

Pau Chung Leng and Tengku Intan Suraya Tengku Aziz
Faculty of Built Environment and Surveying, Universiti Teknologi Malaysia, 81310 UTM Johor Bahru, Johor, Malaysia

ABSTRACT

External shading devices play a crucial role in reducing solar radiation entering buildings and are an important strategy for lowering cooling loads in tropical regions with high temperatures, high humidity and intense solar radiation. This study used a combination of field measurements and software simulations to explore the appropriate ratio of overhang shading devices for a faculty office at Universiti Teknologi Malaysia (UTM). By applying the appropriate ratio of shading device, the compliance rate of indoor air temperature (IAT) in the test room can be brought into compliance with the requirement. Building on this, the study simulated the data of IAT and daylight factor (DF) for four common types of external shading devices across 16 building orientations to identify the appropriate shading device for each orientation. This study found that the most suitable shading device for the -45° building orientation (North-west) is the egg crate shading device. Applying it at an appropriate ratio increased compliance rate of IAT of the test room by 20.7%. This study can provide data and theoretical support for the design and practice of shading devices for buildings in tropical regions such as Malaysia.

Article History

Received : *19 September 2025*
Received in revised form : *29 January 2026*
Accepted : *12 June 2026*
Published Online : *02 September 2026*

Keywords:

Shading devices, Faculty office building, Tropical region, Indoor environmental performance, Building orientations

Corresponding Author Contact:

pengjian@graduate.utm.my

DOI: 10.11113/ ijbes.v13.n3.1684

1. Introduction

Increased energy consumption in buildings for space cooling, due to the phenomenon of overheating (Su et al., 2021). Many researchers focus on office buildings because their current energy performance is poor and they have large potential for energy saving (Chai et al., 2020). Research on office buildings has largely focused on conventional office skyscrapers, which typically have high occupancy and fixed, continuous working hours. However, faculty offices in educational institutions—characterized by low occupancy and irregular working hours—may exhibit lower energy efficiency. And buildings in the tropics are more prone to overheating due to high temperatures, high humidity and intense solar radiation (Gamero-Salinas et al., 2020). Shading devices can mitigate overheating by blocking solar radiation from entering the room, thus reducing energy consumption. There is a study that indicated that small optimizations of shading devices in the tropics can significantly improve the energy performance of buildings (Koç & Maçka Kalfa, 2021). A study conducted in the Metro Manila area shows that using optimized shading devices in tropical regions can improve indoor comfort. It can also support long-term energy saving and sustainable development (Tayag & Conejos, 2025). Therefore, exploring appropriate shading devices for faculty office buildings in the tropics is essential to mitigate overheating and reduce energy consumption.

The main purpose of shading devices is to shade a building against the sun. The performance of shading devices is affected by factors such as solar intensity, the solar path, and the orientation of the windows (Rana et al., 2022a). And shading depends entirely on the location of the sun in the sky (Rana et al., 2022a). This is because the timing and duration of solar radiation varies with the sun's position in the sky. Therefore, each building orientation should be paired with corresponding appropriate shading devices. Using the appropriate shading device ensures the shading system performs at its best—minimizing solar heat gain, lowering indoor air temperature, enhancing indoor environmental performance, and ultimately reducing the energy consumption of the building.

Shading devices can be divided into different types according to different classifications. However, all shading devices can be divided into external and internal shading devices according to the location, and into fixed and dynamic shading devices according to the mode of operation. Internal shading devices also minimize heat exchange between the indoor and outdoor environments, thus reducing energy consumption (Rana et al., 2021). However, compared with internal shading devices, external shading devices are a more effective type of shading device (Zheng et al., 2025). Although dynamic shading systems are garnering more research attention due to their high investment prices, complex design techniques, and operational energy requirements, fixed shading devices remain the most common kind employed in building design (Koç & Maçka Kalfa, 2021). Therefore, this study will focus on exploring appropriate external fixed shading devices.

Different orientations and different types of shading devices produce different effects. A study in Malaysia showed that adding external shading in different orientations led to different reductions in indoor temperature (Oleiwi & Mohamed, 2022).As shown in Table 1, most of the studies on external shading devices focus on 4 orientations or less, with a maximum of 8 orientations. However, the complexity of the requirements during the actual design and construction of the building can lead to uncertainty in the orientation of the building. In order to meet the practical requirements of a larger number of buildings, this study will explore appropriate shading devices in 16 orientations. In terms of types of shading devices, this study explored four common types of shading devices. The vast majority of shading devices employed in actual buildings can be simplified into these 4 types of shading devices.

Simulation is a powerful and effective method when many parameters need to be considered to predict or determine the best solution (Rana et al., 2021). It can also be seen from Table 1 that 17 of the 20 studies used only simulation, two used only field measurements, and only one study used a combination of field measurements and simulation for data collection. Field measurements have the advantage of being realistic and accurate but the generalisability of their results is limited and they are weather dependent. Simulation allows rapid exploration of many scenarios that are impractical or impossible to measure in the real world, such as different orientations. However, simulations have the disadvantage that realism is unpredictable. Therefore, this study uses a combination of field measurements and simulations. Field measurement provides reliable, real-world data that serves as a benchmark for simulation, which in turn allows for broad, flexible exploration of shading devices performance.

The novelty of this study lies in three main aspects. First, this study focuses on faculty office buildings, a building type that has received less attention in previous studies, to explore their energy saving potential. Second, this study investigates the effectiveness of four common types of shading devices in reducing indoor temperatures across 16 building orientations, expanding the scope of existing studies. Third, this study employs a combined approach of field measurements and simulations, ensuring both the accuracy and reliability of the data while enhancing the generalizability of the findings.

It is hypothesized that using optimized external shading devices in faculty office buildings will keep indoor air temperature and daylight factor within a suitable range. Compared with offices without optimized shading devices, this will reduce the use of mechanical cooling systems such as air conditioning and finally lower the building's energy consumption.

Table 1 Research on shading devices from 2020 to 2025

Cite Research	Year	Field Measurement	Simulation	Orientations
(Huo et al., 2020)	2020	√		1
(Settino et al., 2020)	2020		√	4
(Alwetaishi et al., 2021)	2021	√	√	3
(Alajmi et al., 2021a)	2021		√	4
(Koç & Maçka Kalfa, 2021)	2021		√	3
(Eltaweel et al., 2021)	2021		√	1
(Do & Chan, 2021)	2021		√	1
(Wang et al., 2022)	2022		√	4
(Valitabar et al., 2022)	2022		√	1

(Abdelwahab & Sobh, 2022)	2022		√	4
(Rana et al., 2022b)	2022		√	4
(Mohammed et al., 2022)	2022		√	1
(Mangkuto et al., 2022)	2022		√	4
(Dev & Saifudeen, 2023)	2023		√	4
(Baghoolizadeh et al., 2023)	2023		√	1
(Alsukkar et al., 2023)	2023		√	1
(C et al., 2023)	2023		√	1
(Yao et al., 2024)	2024		√	1
(Tayag & Conejos, 2025)	2025		√	1
(Zheng et al., 2025)	2025		√	1

2. Methodology

2.1 Investigation of Indoor Thermal Performance for Test Room

This study selected an office located on the fourth floor of Block B11, Faculty of Built Environment and Surveying, Universiti Teknologi Malaysia (UTM), Johor Bahru, Malaysia, for field measurements. The test room is equipped with an overhang shading device, and its windows are oriented towards the northwest. The precise coordinates of the test room are 1°33'28.95" N and 103°38'07.34" E. The four-story office building adopts a reinforced concrete beam-and-column structural system. The office ceilings are fitted with mineral fiber ceiling tiles, with a ceiling height of 3.75 m. The operable windows measure 1.70 m × 1.70 m, while the fixed windows facing the corridor are 1.20 m × 1.20 m. Additionally, the door is a hard wood door with dimensions of 1.00 m × 2.10 m. The room's window, equipped with a shading device, faces a parking area with no obstruction from trees or tall buildings. The position of the test room is shown in Figure 1.

Figure 1 Location of the test room (Google map) (Left) and Position of the test room (view from car park) (Right)

The IAT in the test room was measured and recorded from 6:00 a.m. on 19 June 2023 to 8:00 p.m. on 19 July 2023 using the HOBO UX100-011 for this field measurement. The time interval was 15 minutes. The HOBO UX100-011 is a data logger designed for highly accurate air temperature monitoring. The data logger contains a mass memory for storing automatically measured values. The measuring device was placed on a desk with a height of 0.75 m, and its position is shown in Figure 2. The placement point is located within the occupied zone as defined by ASHRAE standards for measuring indoor thermal environmental parameters. According to the standard, the occupied zone is defined as the space between the floor and 1.8 m above the floor, more than 1 meter away from exterior walls or windows, and at least 0.3 m away from interior walls (*ANSI/ASHRAE Standard 55-2013*, n.d.).

2.1.1 Requirements for Indoor Thermal Performance

The acceptable range of indoor air temperatures may vary across people from different regions. The recommend range of IAT in MS 1525: 2019 is between 24 °C and 26 °C, but it is for air-conditioned buildings. A study conducted at Universiti Tun Hussein Onn Malaysia found that most students perceived the indoor environment as thermally comfortable when the indoor temperature ranged between 26.9 °C and 27.4 °C (Abdul Rahim et al., 2024). Furthermore, a recent study involving questionnaires and interviews with Malaysian students indicated that, in naturally ventilated environments, the acceptable temperature range is between 26.0 °C and 30.7 °C (Abuelnuor et al., 2021).

Due to significant physiological and psychological differences among individuals, some studies define a comfortable indoor environment as one in which at least 80% of occupants perceive it as comfortable. According to (BSEEP Passive Design Guidebook Final, 2013), some thermal comfort models use a minimum standard of thermal comfort where at least 80% to 90% of participants feel comfortable. Based on the reviewed studies and the specific context of this research, the indoor thermal performance requirement is defined as maintaining the indoor air temperature between 26 °C and 30.7 °C for at least 80% of the working hours between 9:00 a.m. and 6:00 p.m.

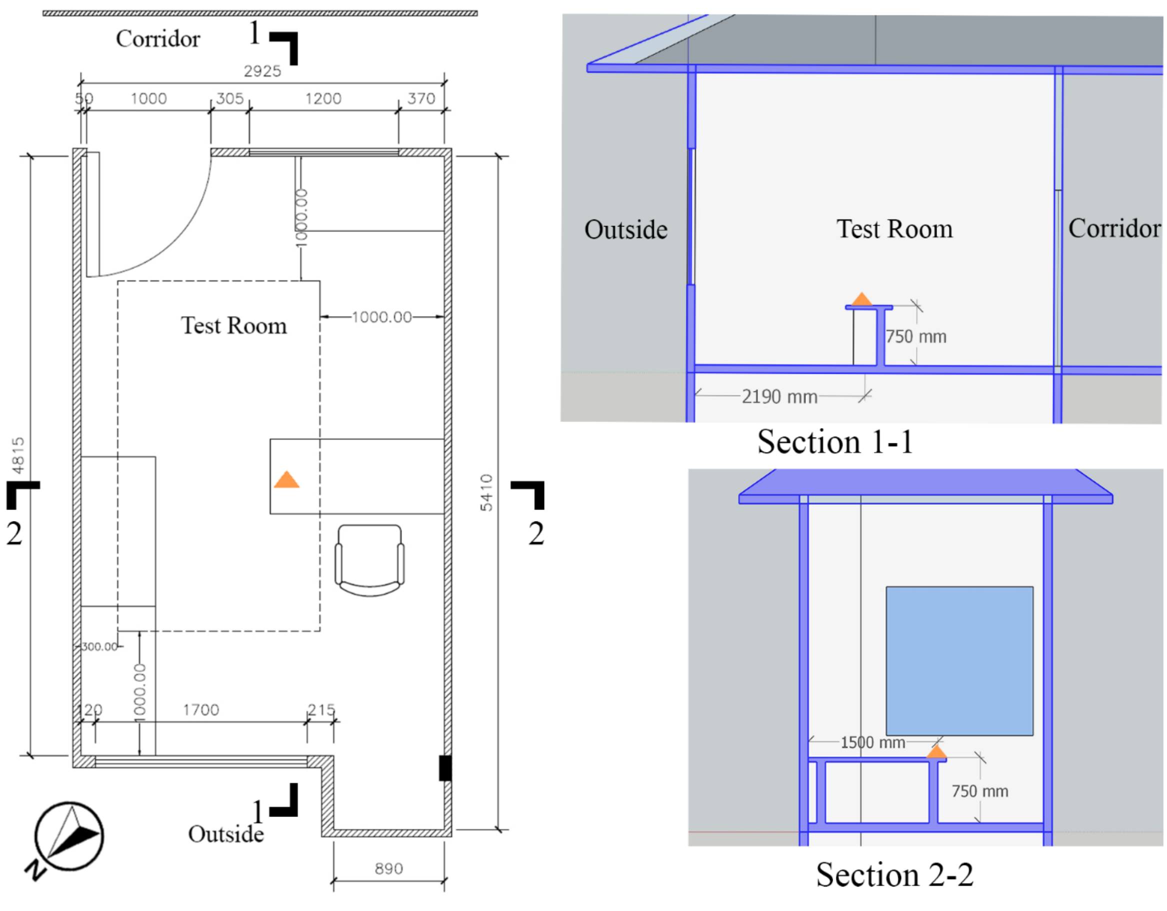

Figure 2 Position of measurement equipment (▲)

2.2 *Exploration of Appropriate Shading Devices for Test Room*

2.2.1 Requirements for Indoor Thermal Performance

This study integrates the modeling software SketchUp and OpenStudio with the EnergyPlus simulation engine. SketchUp Pro 2022 is used to draw and create the geometric form of the model, while OpenStudio 1.5.0 (2023) is employed to modify model properties such as construction and materials. Subsequently, EnergyPlus 22.2.0 (2023) is used to simulate and calculate IAT and Daylight Factor (DF). The workflow for this process is illustrated in Figure 3.

As shown in the figure above, the SketchUp modeling process utilizes basic architectural information such as floor plan dimensions, door and window sizes, and shading device dimensions. Detailed parameters related to building construction and materials are then imported into OpenStudio to ensure that the model closely reflects real conditions. Finally, the building's location and local weather data are imported into EnergyPlus to simulate and generate IAT and DF data for the test room. The SketchUp model of the test room is shown in Figure 4. Table 2 presents detailed information on the test room's construction and materials, while Figure 5 displays the weather data for the test room's location.

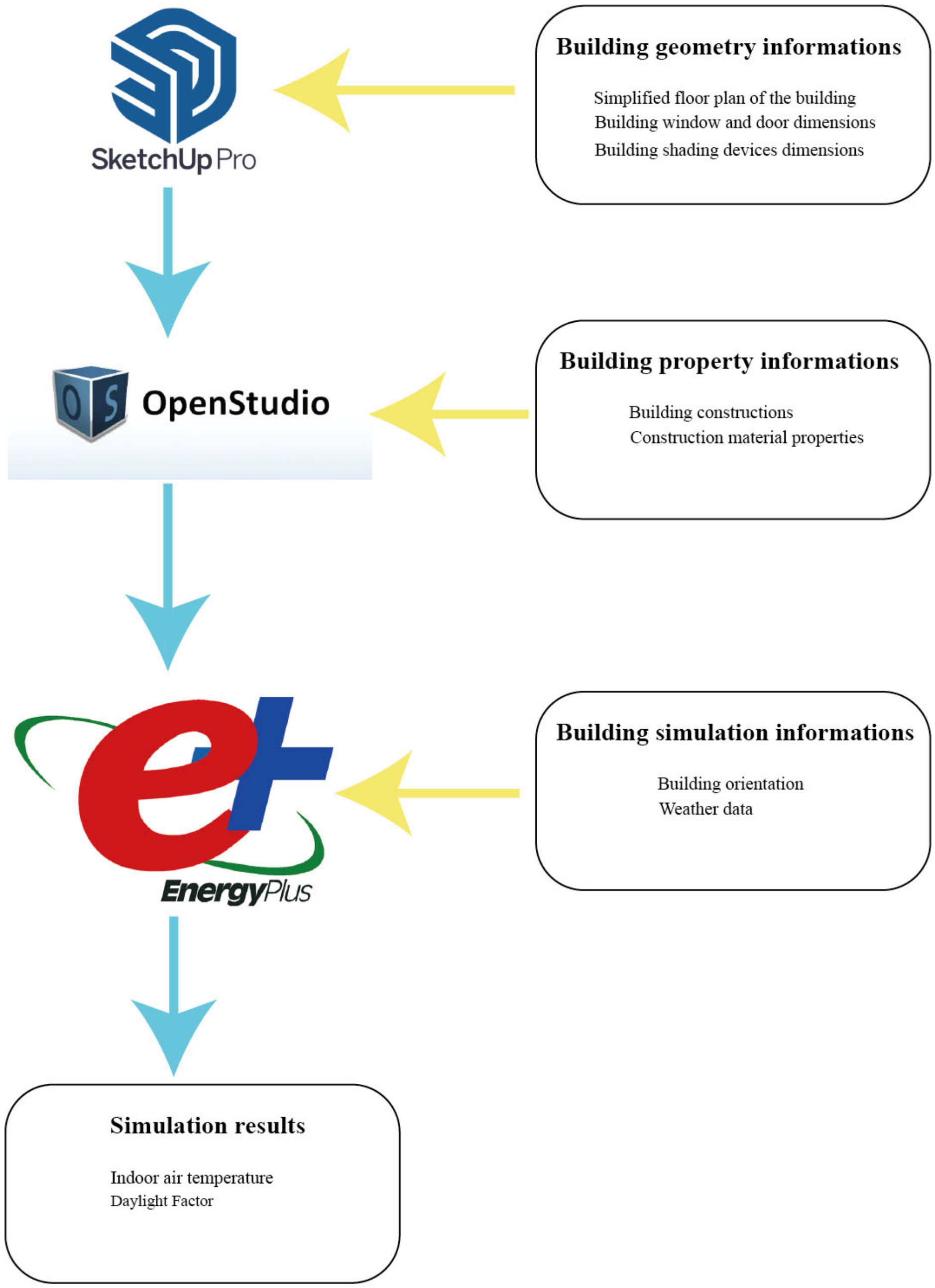

Figure 3 Research operational flow

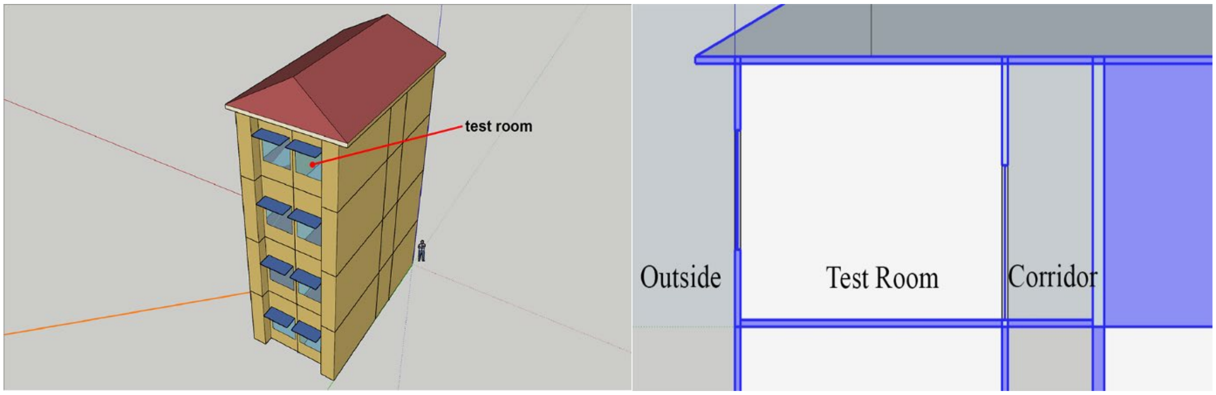

Figure 4 3D model of test room (The orange lines in the figure represent the north direction) (Left) and Section view (Right)

Table 2 Detailed parameters of the construction and materials for the test room

Element	Material	Thickness (mm)	Thermal conductivity (W/m·K)	Density (kg/m³)	Specific heat (J/kg·K)
Wall	gypsum plaster	12	0.42	1200	837
	brick	75	0.721	1700	800
	gypsum plaster	12	0.42	1200	837
Floor	reinforce concrete	100	2.6	2500	750
	mineral fibre tiles	16	0.052	280	840
Roof	gypsum plasterboard	10	0.16	950	840
	fibre glass insulation	50	0.05	36	840
	clay roof tile	15	0.84	1900	800
Ceiling	mineral fibre tiles	16	0.052	280	840
	reinforce concrete	100	2.6	2500	750
	fibre glass insulation	25	0.05	36	840
Door	hard wood	25	0.158	721	1255
Windows	single glass	3	0.9	-	-
Shading Device	concrete	50	0.5	2400	1050

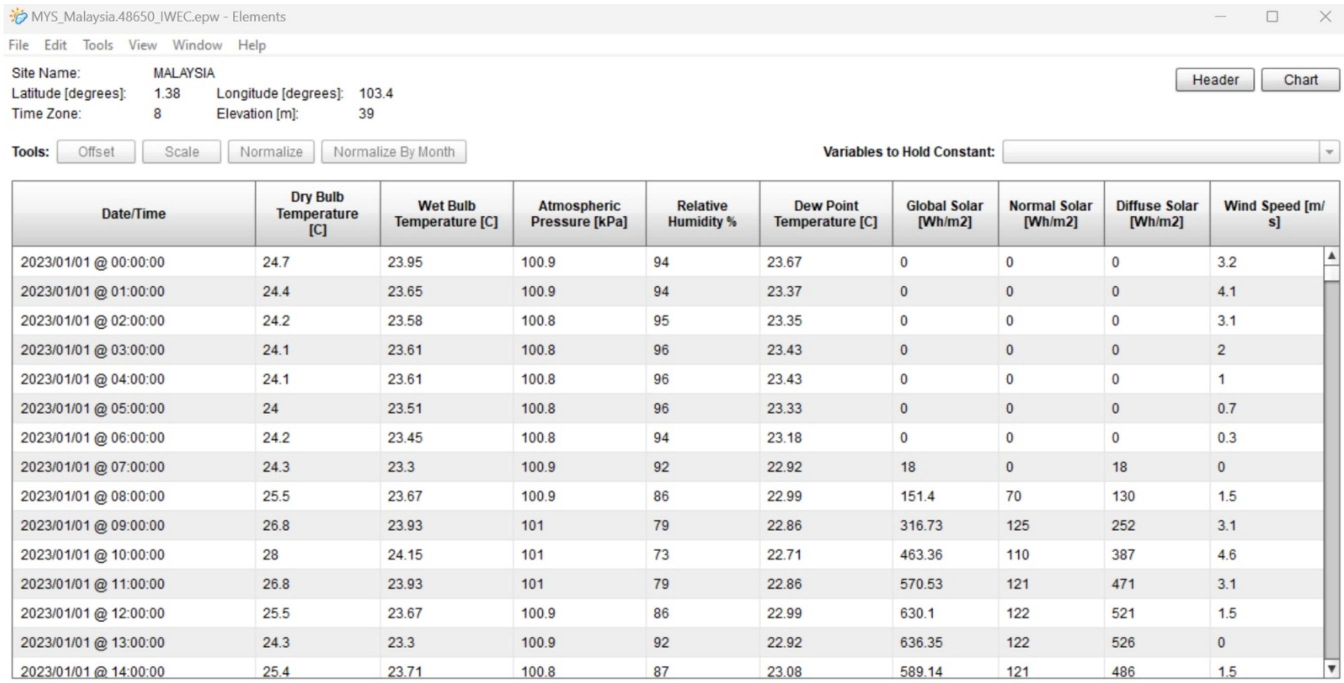
MYS_Malaysia.48650_IWEC.epw - Elements

File Edit Tools View Window Help

Site Name: MALAYSIA
Latitude [degrees]: 1.38 Longitude [degrees]: 103.4
Time Zone: 8 Elevation [m]: 39

Header Chart

Tools: Offset Scale Normalize Normalize By Month

Variables to Hold Constant:

Date/Time	Dry Bulb Temperature [C]	Wet Bulb Temperature [C]	Atmospheric Pressure [kPa]	Relative Humidity %	Dew Point Temperature [C]	Global Solar [Wh/m2]	Normal Solar [Wh/m2]	Diffuse Solar [Wh/m2]	Wind Speed [m/s]
2023/01/01 @ 00:00:00	24.7	23.95	100.9	94	23.67	0	0	0	3.2
2023/01/01 @ 01:00:00	24.4	23.65	100.9	94	23.37	0	0	0	4.1
2023/01/01 @ 02:00:00	24.2	23.58	100.8	95	23.35	0	0	0	3.1
2023/01/01 @ 03:00:00	24.1	23.61	100.8	96	23.43	0	0	0	2
2023/01/01 @ 04:00:00	24.1	23.61	100.8	96	23.43	0	0	0	1
2023/01/01 @ 05:00:00	24	23.51	100.8	96	23.33	0	0	0	0.7
2023/01/01 @ 06:00:00	24.2	23.45	100.8	94	23.18	0	0	0	0.3
2023/01/01 @ 07:00:00	24.3	23.3	100.9	92	22.92	18	0	18	0
2023/01/01 @ 08:00:00	25.5	23.67	100.9	86	22.99	151.4	70	130	1.5
2023/01/01 @ 09:00:00	26.8	23.93	101	79	22.86	316.73	125	252	3.1
2023/01/01 @ 10:00:00	28	24.15	101	73	22.71	463.36	110	387	4.6
2023/01/01 @ 11:00:00	26.8	23.93	101	79	22.86	570.53	121	471	3.1
2023/01/01 @ 12:00:00	25.5	23.67	100.9	86	22.99	630.1	122	521	1.5
2023/01/01 @ 13:00:00	24.3	23.3	100.9	92	22.92	636.35	122	526	0
2023/01/01 @ 14:00:00	25.4	23.71	100.8	87	23.08	589.14	121	486	1.5

Figure 5 Weather data recorded at the weather station at Senai International Airport in Johor Bahru

2.2.2 Validation Results

In this study, the simulation was conducted to generate data on indoor air temperatures at 15-minute intervals between 9 a.m. and 7 p.m. on 21 June 2023, and this data was then compared with data obtained from field measurements to validate the accuracy of the model and simulation software. Some studies have adopted Root Mean Square Error (RMSE) and Mean Bias Error (MBE) to determine the closeness between simulated results and field measurements. A study investigating solutions to glare issues during daytime fire evacuation in Malaysian office buildings employed RMSE and MBE to validate the similarity between simulation outputs and on-site data (Aw et al., 2023). Another study, which optimized building energy consumption using a dynamic shading system, also utilized RMSE and MBE to assess the discrepancy between simulated and measured results during daylighting control analysis (Kunwar et al., 2021). In addition, a study using EnergyPlus to explore façade design for indoor air temperature and cooling loads in buildings in tropical regions also used RMSE and MBE to validate the simulation results (Tong et al., 2021). The equations for RMSE and MBE are shown as follow:

$$\text{RMSE }(\%)=\frac{\sqrt{\frac{1}{n}\sum_{i=1}^{n}(S_i-A_i)^2}}{\sum_{i=1}^{n}A_i/n}\times 100,$$

$$\text{MBE }(\%)=\frac{\sum_{i=1}^{n}(S_i-A_i)}{\sum_{i=1}^{n}A_i}\times 100,$$

Where Si represents the value from simulation, Ai represents the value from field measurement, n represents number of measurements.

The RMSE and MBE of the simulated IAT in the test room from 9am to 6pm on 21 June 2023 are summarised in Table 3. A number of studies validating models and simulation accuracy have indicated that simulation results are sufficient to meet the ASHRAE standards when the MBE is within ±10% and the RMSE is below 30% (Aw et al., 2023; Tong et al., 2021). In this study, both the values of RMSE and MBE are less than 10%, so the accuracy of the model and simulation meets the requirements and the model can be used for simulation in the subsequent process of this study.

2.2.3 Requirements for Appropriate Shading Devics

After the validity of the model and simulation software is validated, the model will be used to simulate the IAT and DF of the test room with different ratios of overhanging shading devices. The simulation results will be analysed to determine the appropriate ratio of overhanging shading devices for the test room and compared with the current indoor thermal performance of the test room to determine the feasibility of adjusting the shading devices to improve the indoor environmental performance. The model used to explore the appropriate ratio of overhang shading device for the test room is shown in Figure 6.

Table 3 Comparison between simulation and field measurement

Date	Time (hour)	RMSE (%)	MBE (%)
21/06/2023	09:00	7.90	7.85
	10:00	7.65	7.61
	11:00	7.89	7.84
	12:00	6.98	6.95
	13:00	6.21	6.16
	14:00	6.20	6.16
	15:00	5.79	5.79
	16:00	7.66	7.64
	17:00	7.81	7.80
	18:00	8.15	8.13

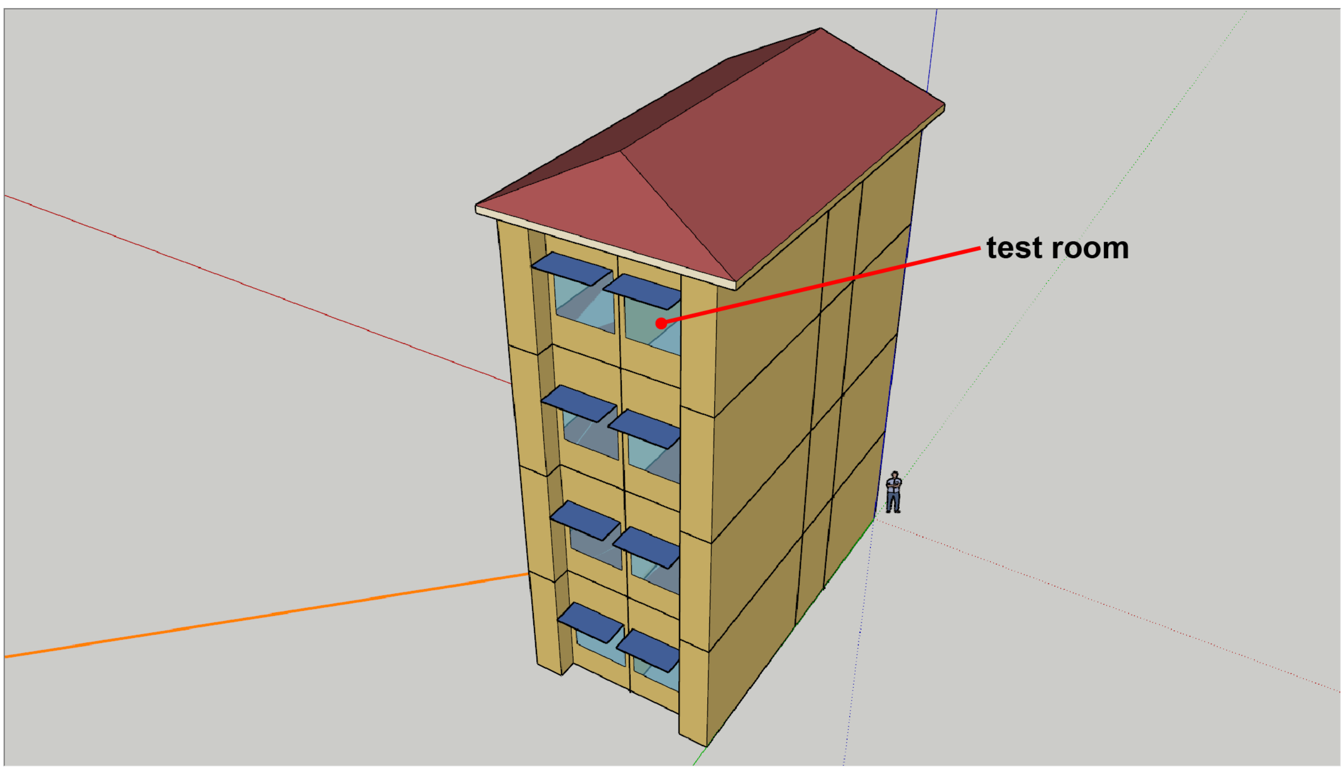

Figure 6 SketchUp model of test room with shading device (The orange lines in the figure represent the north direction)

In tropical regions, indoor air temperatures are generally high, and increasing the ratio of shading devices may significantly improve indoor thermal performance. However, an excessive ratio of shading device can lead to poor indoor daylight performance. Therefore, DF is introduced as an additional evaluation metric when determining the appropriate ratio of shading device for the test room and, subsequently, for identifying appropriate shading devices across the 16 orientations. DF provides a direct method for describing the distribution, penetration, and intensity of daylight within space, as referenced in MS1525:2019. The recommended range of DF in MS1525:2019 is shown in Figure 7.

DF (%)	Lighting	Glare	Thermal comfort	Appearance and energy implication
> 6.0	Intolerable	Intolerable	Uncomfortable	Room appears strongly day lit. At daytime artificial lighting is rarely needed, but thermal problems due to solar heat gain and glare may occur.
3.5 - 6.0	Tolerable	Uncomfortable	Tolerable	
1.0 - 3.5	Acceptable	Acceptable	Acceptable	Room appears moderately day lit. Good balance between lighting and thermal aspects. Supplementary artificial lighting is needed at dark areas due to effect of layout or furniture arrangement
< 1.0	Perceptible	Imperceptible	Acceptable	Room looks gloomy, artificial lighting is needed most of the time.
NOTE. In Malaysia, DF between 1.0 and 3.5 is recommended.				

Figure 7 Range of DF in Table 1 of MS 1525

In summary, the requirement for determining the appropriate ratio of shading device for the test room, as well as for identifying appropriate shading devices across the 16 orientations is that on the four key days of the year—spring equinox, summer solstice, autumn equinox, and winter solstice—between 9:00 a.m. and 6:00 p.m., at least 80% of the time the IAT should fall within the range of 26 °C to 30.7 °C, and the DF should range between 1% and 6%.

2.3 Identification of Appropriate Shading Devices for Different Orientations

After determining the impact of appropriate shading devices in improving indoor environmental performance, this study uses the validated model to simulate IAT and DF for four types of shading devices, each applied with varying ratios across 16 orientations. The goal is to identify the appropriate type and ratio of shading device for each orientation. Most of the external shading devices can be simplified into four fundamental types: overhang, side fins, overhang with side fins, and egg-crate shading devices. Furthermore, due to the complexity of architectural practice, building orientations can vary widely. However, dividing orientations at 22.5° intervals into 16 directions allows for broader coverage and applicability across a wider range of building orientations. Therefore, the findings of this study are broadly applicable and widely generalizable. The models of the four types of shading device are shown in Figure 8 and Figure 9, and the 16 orientation divisions are illustrated in Figure 10.

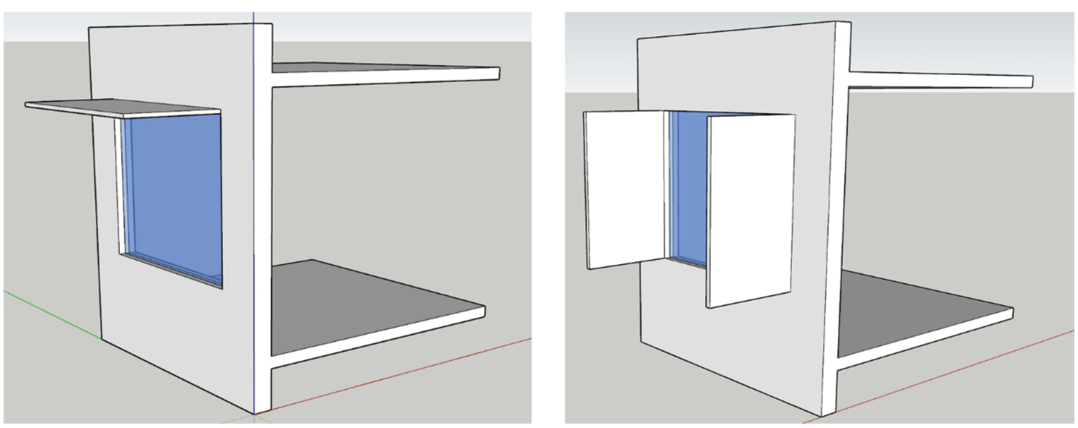

Figure 8 Model of overhang shading device (Left) and Model of side fins shading device (Right)

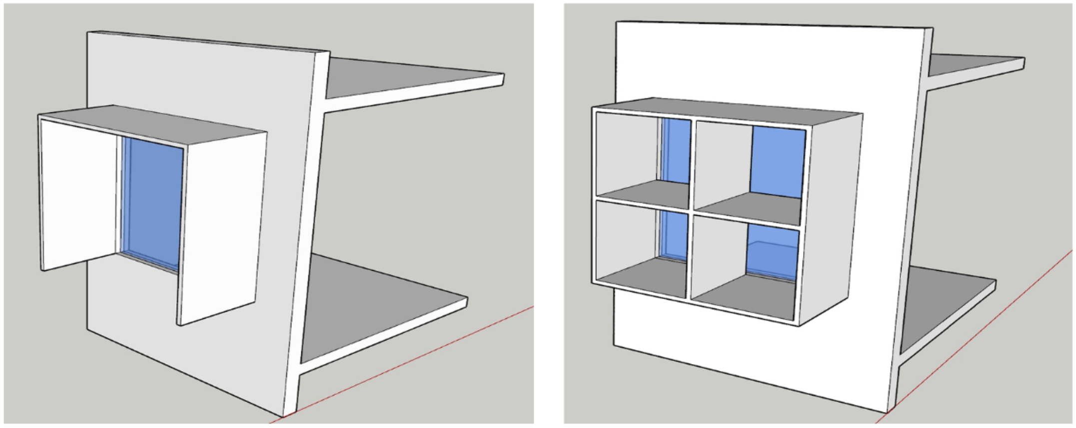

Figure 9 Model of overhang with side fins shading device (Left) and Model of egg-crate shading device (Right)

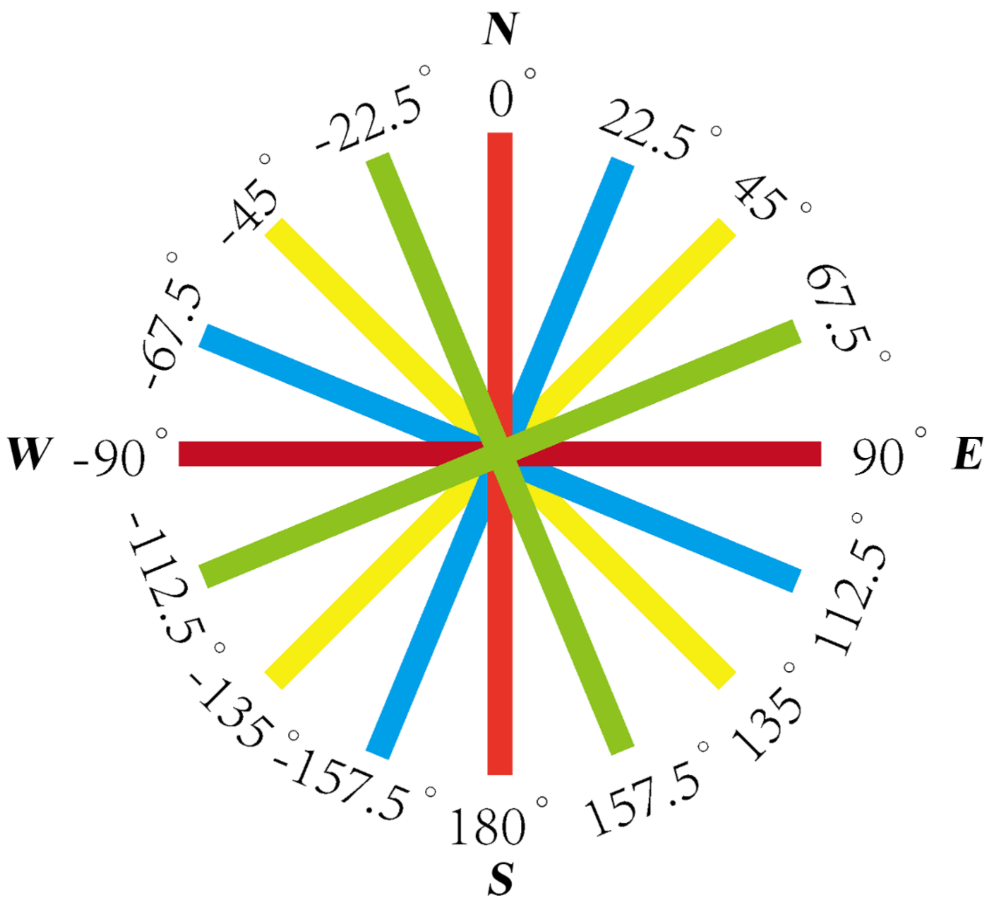

Figure 10 Schematic diagram of the 16 orientations

2.3.1 Calculation of the Ratio Of Shading Devices

The ratio of an external shading device typically refers to the proportion of the device's dimensions (such as depth, width, or projection) relative to the window it is shading. This ratio is crucial in determining the effectiveness of the shading device in reducing solar heat gain. The following are the calculation methods for determining the ratios of the four types of devices explored in this study: overhang, side fins, overhang with side fins and egg-crate shading devices.

The ratio for overhang shading devices is the ratio of depth to height. Depth is measured from the exterior surface of the window to the outermost edge of the device, as indicated by D_h in Figure 11. Height is measured from the underside of the device to the bottom of the window, as indicated by H in Figure 11. The equation is as below: $R_h = D_h / H$, Where R_h is the horizontal ratio of shading device, D_h is measured from the exterior surface of the window to the outermost edge of the device, and H is measured from the underside of the device to the bottom of the window.

The ratio for side fins shading devices is the ratio of depth to width. Depth is measured from the exterior surface of the window to the outermost edge of the device, as indicated by D_v in Figure 11. Width is the width or span between vertical devices, as indicated by W in Figure 11. The equation is as below: $R_v = D_v / W$, Where R_v is the vertical ratio of shading device, D_v is measured from the exterior surface of the window to the outermost edge of the device, and W is the width or span between vertical devices.

Overhang with shading devices and egg-crate shading devices are all combined shading devices. The calculation of the combined shading device's ratio is divided into two parts: the horizontal ratio (R_h) and the vertical ratio (R_v). The methods for calculating these two ratios are the same as those described earlier for overhang shading device and side fins shading device.

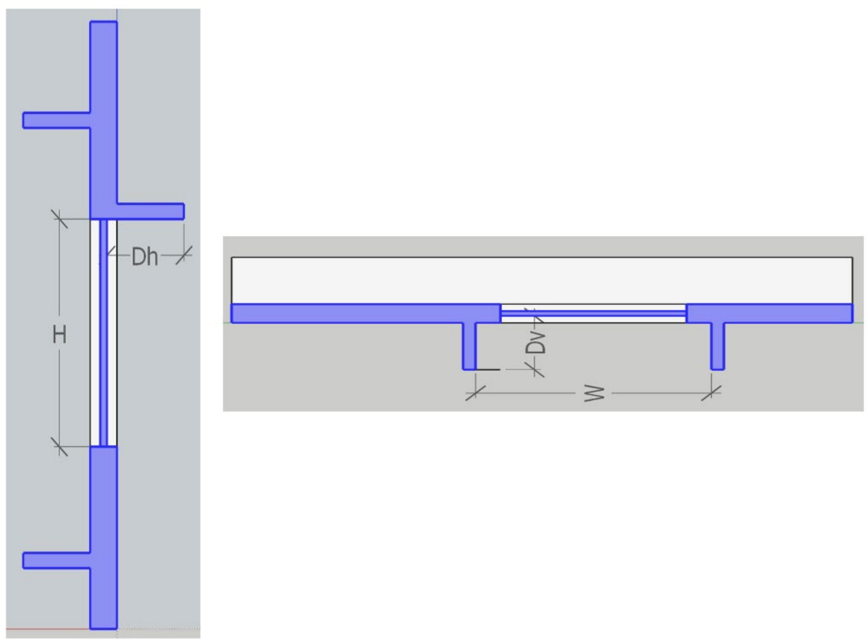

Figure 11 Ratio of overhang shading device (Left) and Ratio of side fins shading device (Right)

2.3.2 Calculation of the ratio of shading devices

If the DF for all 16 orientations fails to meet the requirement at a certain ratio, this study will not proceed with simulating larger ratios for that type of shading device. As the ratio of shading devices increases, more daylight entering the room will be blocked and the percentage of time that DF meets the requirement will decrease. The suitable ratio ranges for the four types of shading devices across 16 building orientations are presented in Figures 12, 13, 14, and 15 respectively. As illustrated in the figure, the DF compliance rate drops below 80% across all 16 orientations when the ratio reaches 1.3 for the overhang shading device, 1.5 for the side fins shading device, 1.0 for the overhang with side fins shading device, and 0.6 for the egg-crate shading device. Therefore, the ratios simulated in this study range from 0.1 to 1.3 for overhang shading devices, 0.1 to 1.5 for side fins shading devices, 0.1 to 1.0 for overhang with side fins shading devices, 0.1 to 0.6 for egg crate shading devices. All shading device types are evaluated at intervals of 0.1.

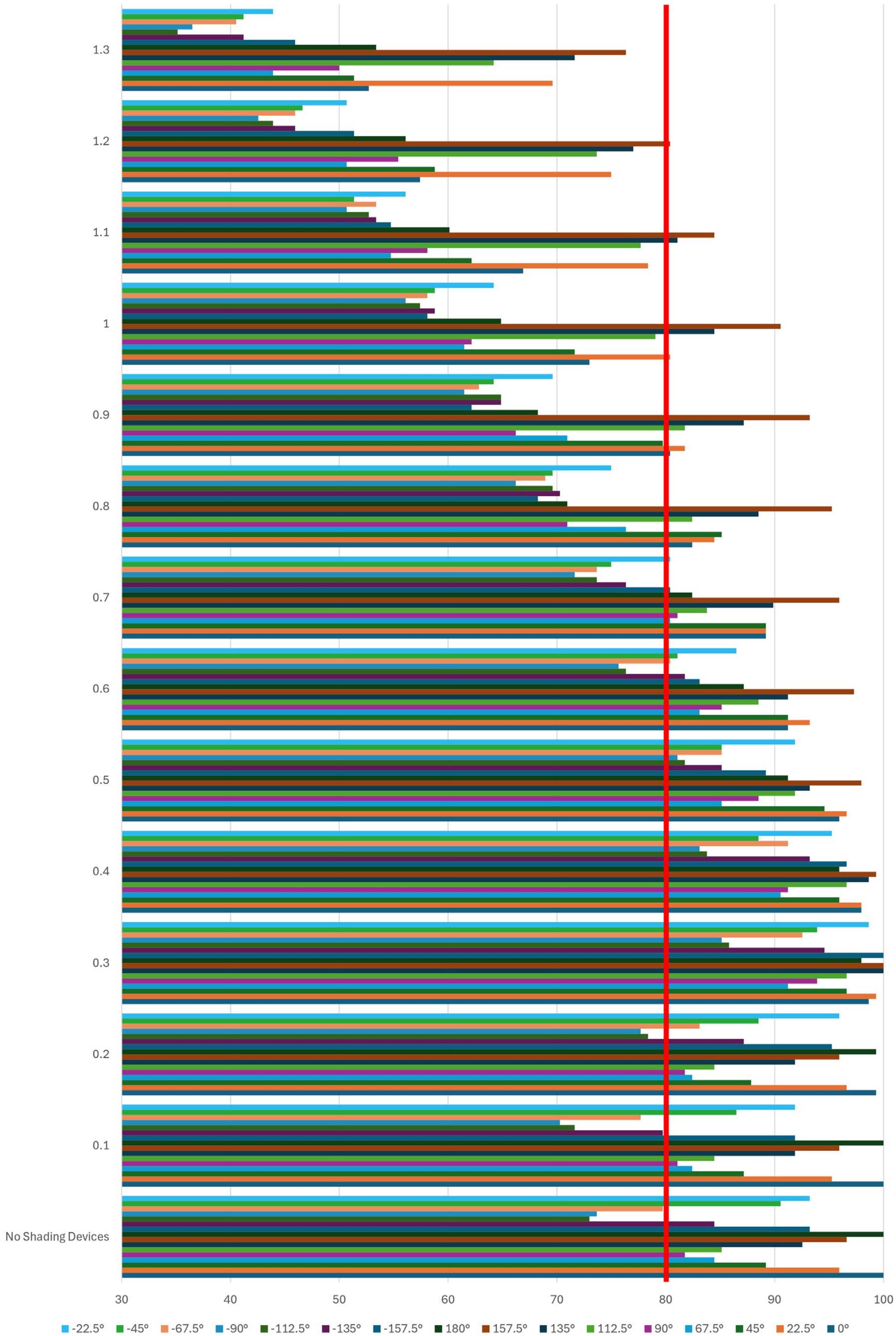

Figure 12 Compliance rate of DF for overhang shading devices with different ratios across 16 building orientations

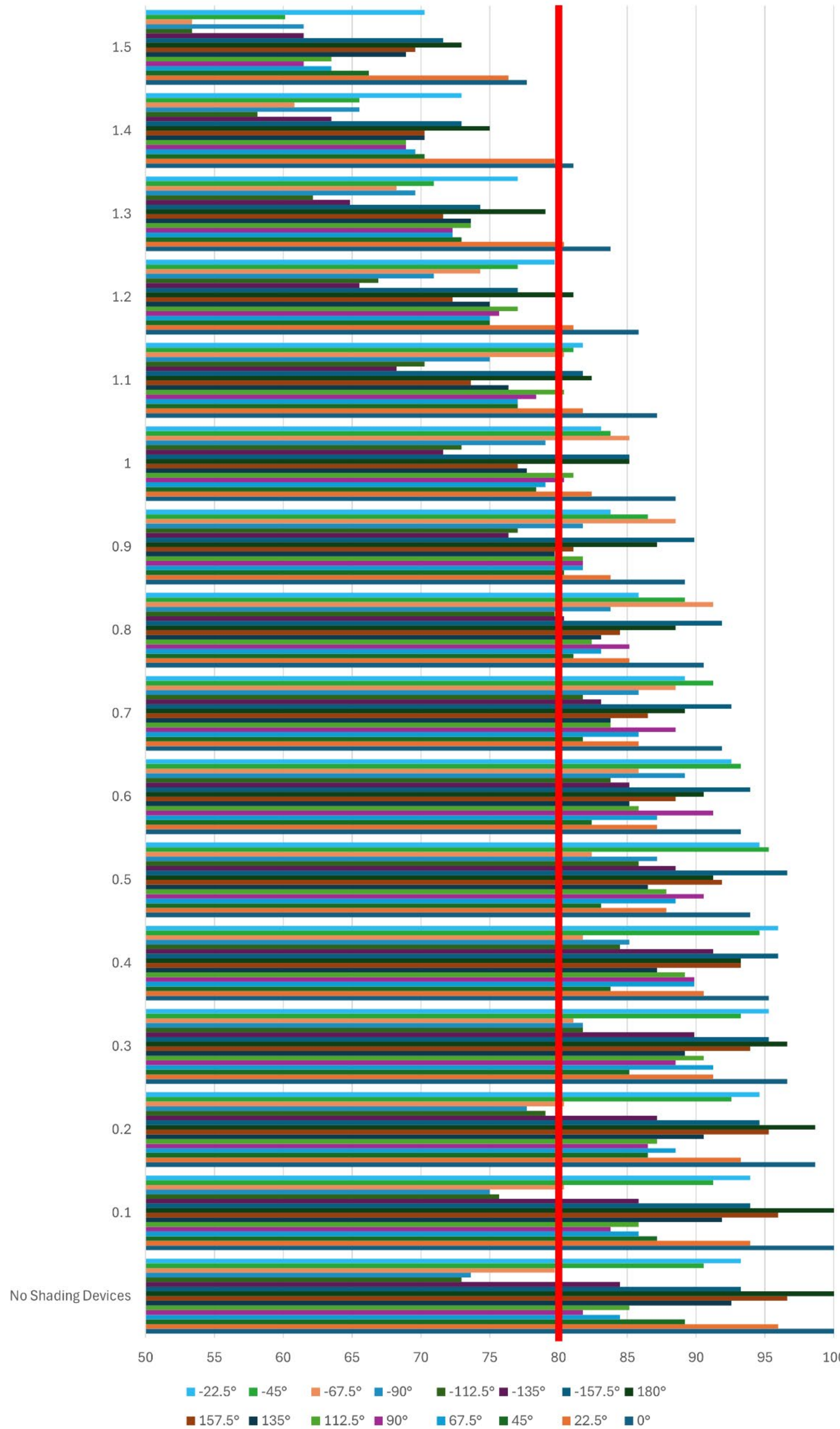

Figure 13 Compliance rate of DF for side fins shading devices with different ratios across 16 building orientations

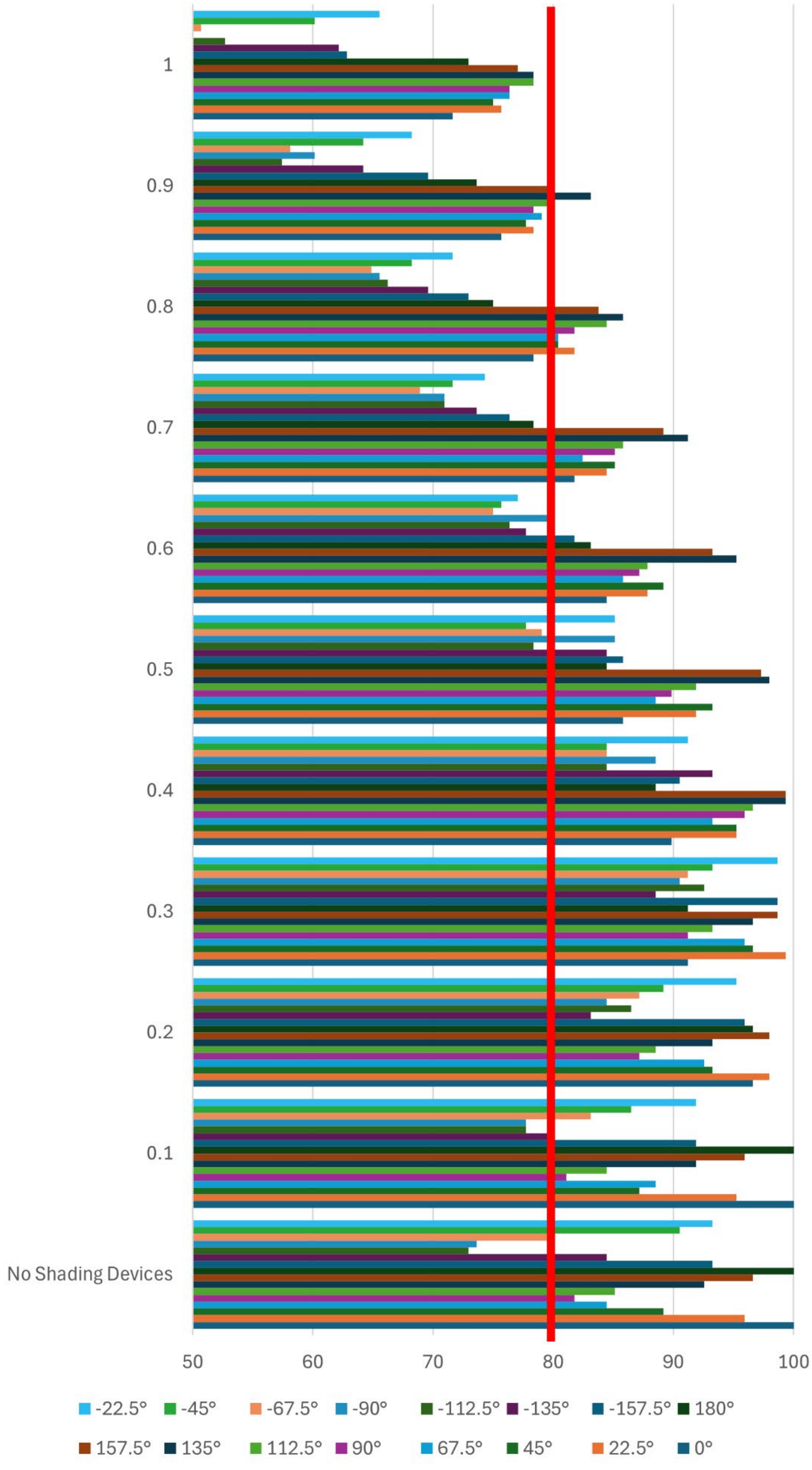

Figure 14 Compliance rate of DF for overhang with side fins shading devices with different ratios across 16 building orientations

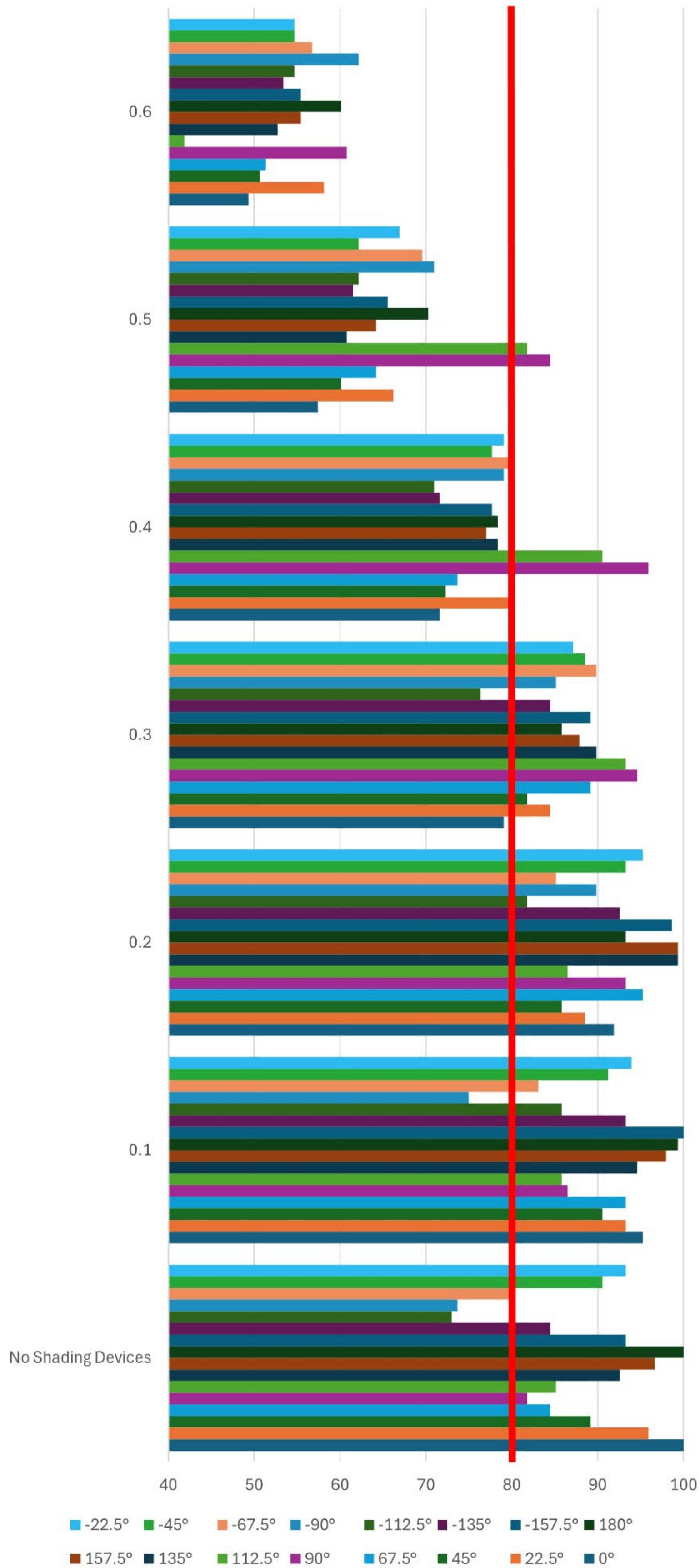

Figure 15 Compliance rate of DF for egg-crate shading devices with different ratios across 16 building orientations

3. Results

3.1 Current Status of Indoor Thermal Performance

This study conducted field measurements of IAT in a typical faculty office within the study area from June 19 to July 19, 2023. Data was recorded every 15 minutes between 9:00 a.m. and 6:00 p.m. daily, providing a reliable reflection of the test room's indoor thermal performance. The results of the field measurements are shown in Figure 16.

As shown in Figure 16, the IAT in the test room ranged between 26.32 °C and 34.65 °C from June 19 to July 19, 2023, during the daily period from 9:00 a.m. to 6:00 p.m. The highest recorded temperature occurred at 6:00 p.m. on June 28, while the lowest was observed at 9:00 a.m. on July 15. The percentage of time during which the indoor air temperature remained within the acceptable range of 26 °C to 30.7 °C was only 72.54%, which fell below the 80% threshold required in this study. Throughout the one-month period from June 19 to July 19, 2023, the IAT in the test room never fell below 26°C between 9:00 a.m. and 6:00 p.m. This indicates that the room consistently experienced elevated temperatures, suggesting a condition of indoor overheating. Because the small ratio of overhang shading device allowed excessive solar radiation to enter the interior. Increasing the overhang shading ratio could help mitigate this over-heating. Further research is needed to explore the appropriate ratio of overhanging shading devices used in the test room so that the compliance rate of IAT in the test room meets the requirements of this study.

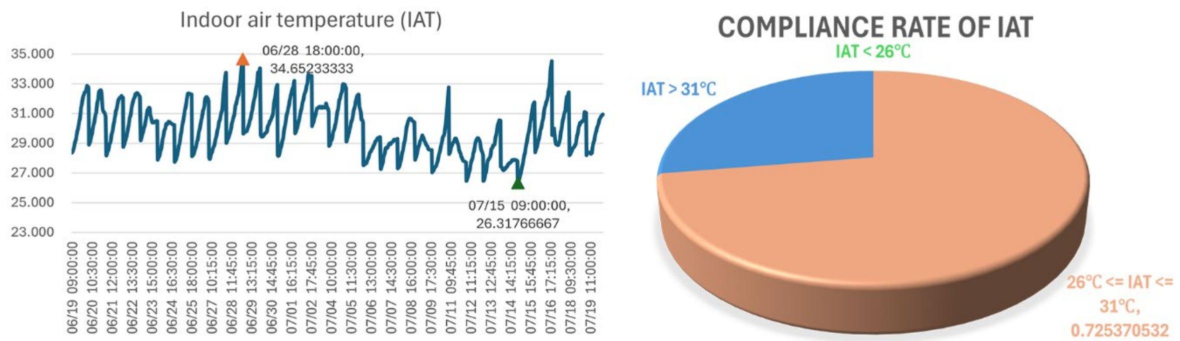

Figure 16 Measured data of IAT for the test room (Left) and Compliance rate of IAT for the test room (Right)

3.2 Appropriate Ratios for Test Room

Based on the previous results, the low ratio of the overhang shading device in the test room resulted in high IAT, that failed to meet the requirements in this study. Therefore, this study proceeds to simulate the indoor air temperature and illuminance levels of the test room with overhanging shading devices using ratios of 0.4 to 1.3 at intervals of 0.1. the requirement for determining the appropriate ratio of shading device is that on the four key days of the year—spring equinox, summer solstice, autumn equinox, and winter solstice—between 9:00 a.m. and 6:00 p.m., at least 80% of the time the IAT should fall within the range of 26 °C to 30.7 °C, and the DF should range between 1% and 6%.

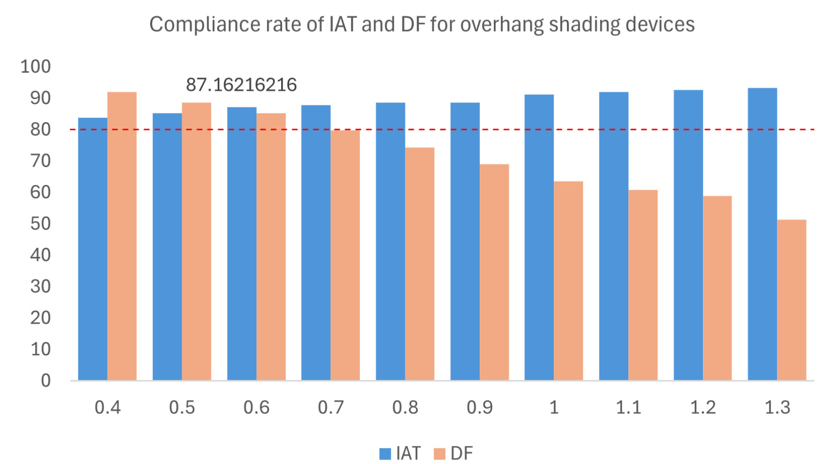

Figure 17 Compliance rate of IAT and DF for overhang shading devices with different ratio on -45° building orientation (Northwest)

As shown in Figure 17, when the ratio of overhang shading device for the northwest-facing test room falls between 0.4 and 0.6, both the IAT and DF compliance rates exceed 80%, meeting the requirements of this study. Therefore, the appropriate ratio of overhang shading device for the test room is identified as 0.4 to 0.6. By applying appropriate ratio of shading device, the compliance rate of IAT in the test room increased from 72.54%, which did not meet the requirements, to 87.16%, which fulfilled the requirements. This demonstrates that appropriate shading devices can indeed enhance the compliance rates of IAT and DF, thereby improving indoor environmental performance.

However, the appropriate ratio of the same type of shading device may be different for different orientations, and the appropriate ratio for different types of shading devices on the same orientation may also be different. To provide practical guidance applicable to a wide range of building scenarios, this study will proceed to use the validated model to simulate IAT and DF data for four common types of shading devices with different ratios across 16 orientations to determine the most suitable shading device for each orientation and the appropriate ratio for each type of shading device.

3.3 Appropriate Shading Device for Different Orientations

3.3.1 Appropriate Shading Devices on 0° Building Orientation

Due to the solar path, the 0° building orientation (north) in Malaysia primarily receive diffuse light, with minimal direct solar radiation. As shown in Figure 18, for overhang shading devices in rooms with a 0° building orientation, the appropriate ratio is between 0 and 0.5. For side fins shading devices in rooms with a 0° building orientation, the appropriate ratio is between 0 and 0.6. For overhang with side fins shading devices in rooms with a 0° building orientation, the appropriate ratio is between 0 and 0.4. Similarly, for egg-crate shading devices in rooms with a 0° building orientation, the appropriate ratio is between 0 and 0.2.

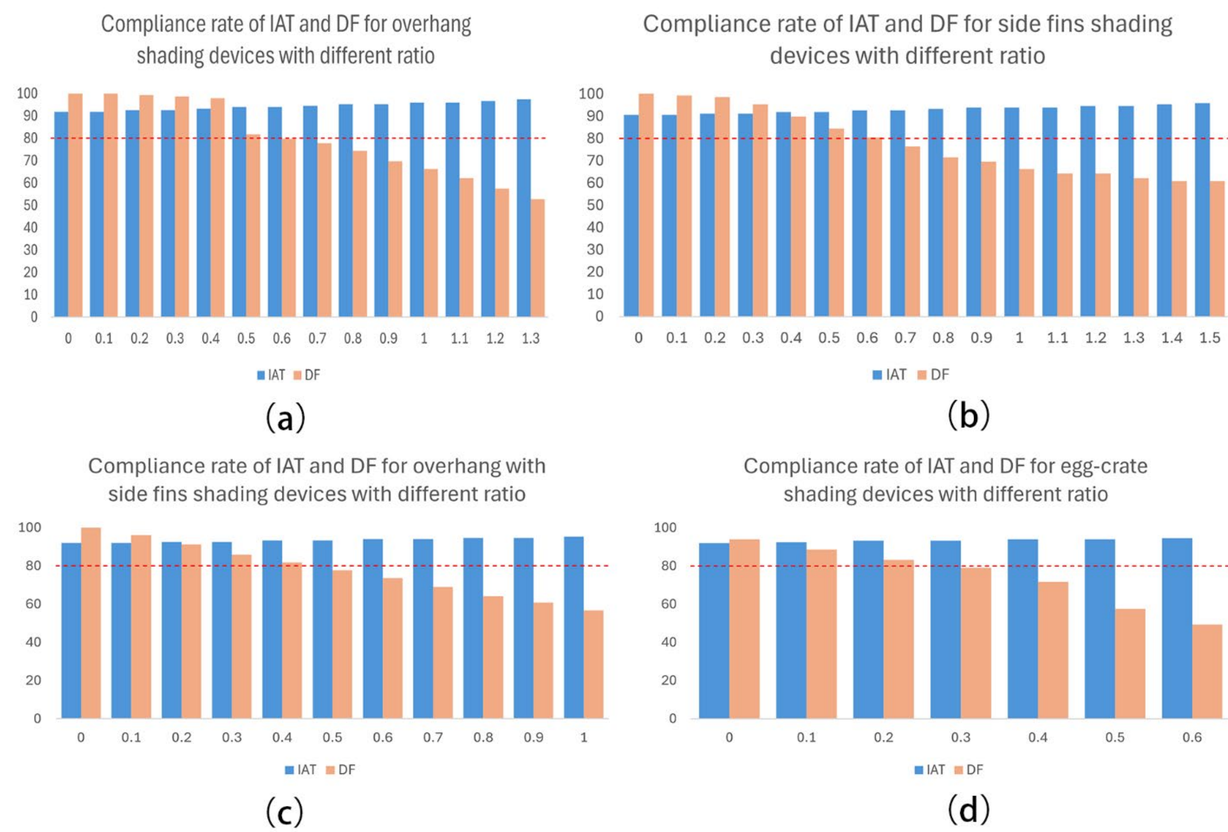

Figure 18 Compliance rate of IAT and DF for four types of shading devices with different ratios on 0° building orientation: (a) overhang shading devices; (b) side fins shading devices; (c) overhang with side fins shading devices; (d) egg-crate shading devices

In buildings, the energy consumed to reduce IAT accounts for the largest share of total energy use. Furthermore, the DF continuously satisfies the necessary standard, guaranteeing visual comfort, provided that the ratio of shading device stays within a appropriate range. Therefore, to identify the most suitable type of shading device for rooms on 0° building orientation, this study compares the maximum IAT compliance rate achieved by each type of shading device when applied within its respective appropriate ratio range.

With a ratio of 0.5, the highest IAT compliance rate for overhang shading devices is 93.92%, as seen in Figure 19. With a ratio of 0.6, side fins shading devices have the highest IAT compliance rate, at 92.57%. With a ratio of 0.4, overhang with side fins shading devices have the highest IAT compliance rate, at 93.24%. Similarly, with a ratio of 0.2, egg-crate shading devices have the highest IAT compliance rate, at 93.24%. Consequently, overhang shading device is the most suitable type of shading devices for 0° building orientation.

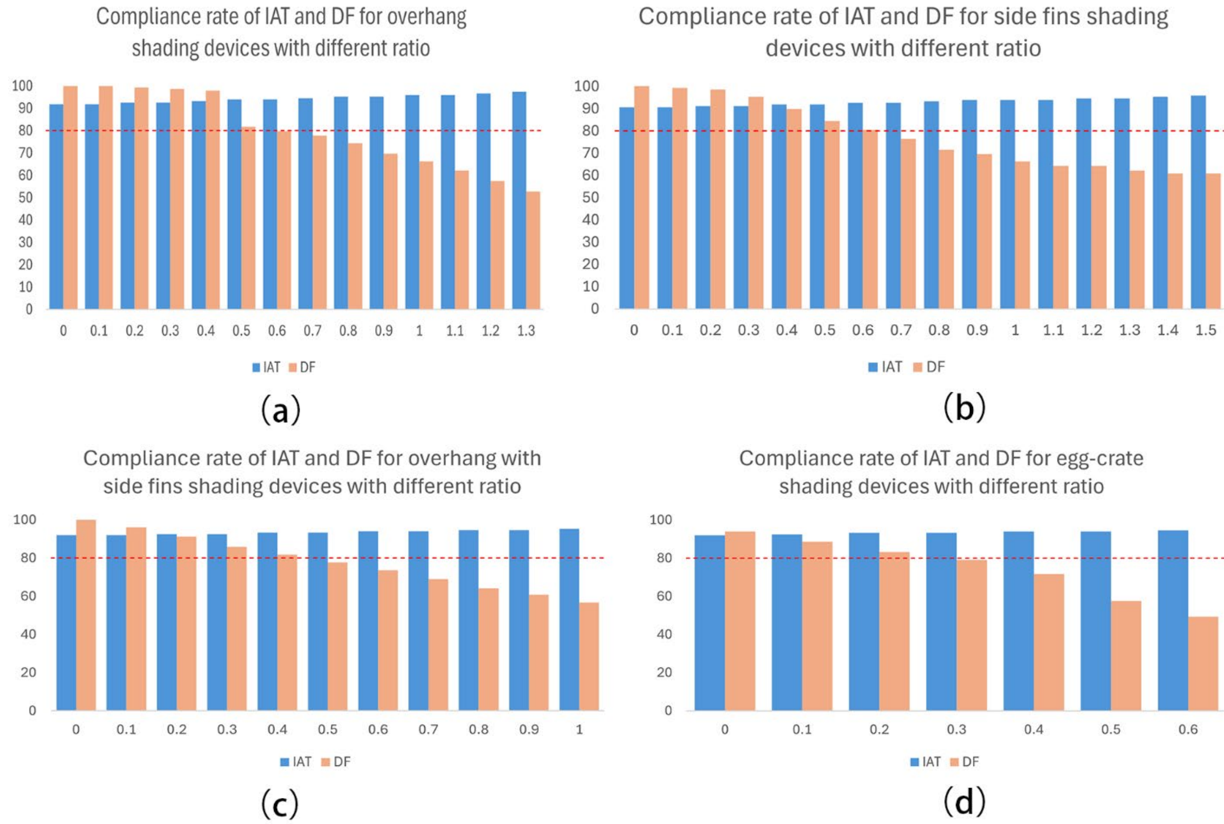

Figure 19 Compliance rate of IAT and DF for four types of shading devices with appropriate ratios on 0° building orientation: (a) overhang shading devices; (b) side fins shading devices; (c) overhang with side fins shading devices; (d) egg-crate shading devices

The remaining 15 building orientations were analysed using the same method as for the 0° building orientation to identify the appropriate ratio for the four types of shading devices. The most suitable type of shading device for each orientation was then identified by comparing the compliance rates for indoor air temperature when using the appropriate ratio of shading devices. The appropriate ratio for the four types of shading devices across 16 building orientations, along with the highest IAT compliance rates for four types of shading devices when using appropriate ratios are summarised in Table 4. Blue text indicates the type of shading device that achieved the highest IAT compliance rate at its appropriate ratio.

Table 4 The appropriate ratio for the four types of shading devices across 16 building orientations and the highest IAT compliance rates for four types of shading devices when using appropriate ratios

Orientations	Overhang Shading Devices	Side Fins Shading Devices	Overhang with Side Fins Shading Devices	Egg-crate Shading Devices
0°	0-0.5; 0.5 (95.32%)	0-0.6; 0.6 (92.57%)	0-0.4; 0.4 (93.24%)	0-0.2; 0.2 (93.24%)
22.5°	0.1-0.6; 0.6 (90.54%)	0.1-0.7; 0.7 (87.84%)	0.1-0.4; 0.4 (88.51%)	0-0.2; 0.2 (89.19%)
45°	0.2-0.6; 0.6 (86.49%)	0.3-0.6; 0.6 (88.51%)	0.2-0.5; 0.5 (90.54%)	0.1-0.3; 0.3 (91.22%)
67.5°	0.3-0.8; 0.8 (88.51%)	0.3-0.7; 0.7 (82.43%)	0.3-0.6; 0.6 (89.19%)	0.2-0.3; 0.3 (87.16%)
90°	0.4-1.0; 1.0 (85.13%)	0.3-0.9; 0.9 (87.16%)	0.4-0.7; 0.7 (90.54%)	0.2-0.4; 0.4 (91.22%)
112.5°	0.5-1.0; 0.9 (91.22%)	0.4-0.8; 0.8 (84.46%)	0.4-0.7; 0.7 (91.22%)	0.2-0.4; 0.4 (97.97%)
135°	0.5-1.0; 0.9 (95.95%)	0.4-0.9; 0.9 (83.78%)	0.4-0.9; 0.9 (95.27%)	0.3-0.4; 0.4 (93.24%)
157.5°	0.5-0.9; 0.9 (99.32%)	0.5-1.1; 1.1 (91.22%)	0.5-0.8; 0.8 (93.92%)	0.2-0.3; 0.3 (94.59%)
180°	0.5-0.9; 0.9 (99.32%)	0.5-1.2; 1.2 (91.22%)	0.4-0.8; 0.8 (95.95%)	0.2-0.3; 0.3 (97.97%)
-157.5°	0.6-1.0; 1.0 (93.92%)	0.6-1.2; 1.2 (92.57%)	0.5-0.9; 0.9 (97.97%)	0.2-0.3; 0.3 (97.30%)
-135°	0.7-1.1; 1.1 (96.62%)	0.7-1.2; 1.2 (91.22%)	0.6-0.9; 0.9 (92.57%)	0.2-0.4; 0.3 (95.95%)
-112.5°	0.7-1.2; 1.2 (91.22%)	0.7-1.1; 1.1 (87.16%)	0.6-0.9; 0.9 (91.89%)	0.3-0.4; 0.4 (91.22%)
-90°	0.7-1.2; 1.2 (91.89%)	0.8-1.1; 1.1 (89.86%)	0.6-0.9; 0.9 (92.57%)	0.3-0.5; 0.5 (96.62%)
-67.5°	0.5-0.8; 0.8 (87.16%)	0.6-0.9; 0.9 (89.86%)	0.5-0.9; 0.9 (93.24%)	0.3-0.5; 0.5 (93.92%)
-45°	0.4-0.6; 0.6 (87.16%)	0.4-0.7; 0.7 (88.51%)	0.3-0.6; 0.6 (88.51%)	0.3-0.4; 0.4 (93.24%)
-22.5°	0.3-0.6; 0.6 (87.16%)	0.4-0.8; 0.8 (87.84%)	0.3-0.7; 0.7 (95.27%)	0.2-0.3; 0.3 (93.24%)

4. Discussion

To facilitate reference and application in architectural practice, this study summarizes the most suitable type of shading device and appropriate ratios for four commonly used types of shading devices for the 16 building orientations in Table 5. Blue text indicates the most suitable type of shading device for that orientation.

Field measurements indicate that using low-ratio overhang shading device at the -45° building orientation is insufficient to block direct solar radiation, resulting in indoor overheating. Simulation results show that increasing the ratio of overhang shading device to an appropriate level improves the compliance rate of IAT to meet the requirement, though it is not the most effective solution available. According to the solar path, shading devices located in the -45° building orientation (north-west) require vertical shading devices to block low-angle lateral solar radiation. The use of unsuitable type of shading devices in the test room also contributed to the unsatisfied IAT. Simulation results show that the most suitable shading device for the -45° building orientation (North-west) is the egg crate shading device. Applying it at an appropriate ratio increases compliance rate of IAT of the test room by 20.7%. This means that a northwest-facing faculty office will not need mechanical cooling systems such as air conditioning for 93.24% of the time when using an egg-crate shading device at a 0.4 ratio. Because faculty offices have low occupancy and irregular usage times, offices with optimized shading devices can greatly reduce the use of air conditioners and fans. This will save a large amount of energy and greatly improve the building's energy efficiency.

At the 0° building orientation, direct solar radiation is minimal throughout the year, making shading devices nonessential. Overhang shading device can effectively block the intense, high-angle solar radiation during midday. The results of this study show that there is little variation in IAT and DF, so shading devices for the 0° building orientation are not necessary, which is consistent with its result. One study comparing overhang shading devices, side fins shading devices and overhang with side fins shading devices in reducing annual building energy consumption showed that overhang with side fins shading devices were more effective than overhanging shading devices in 0°, 90°, 180°, -90° building orientations (Alajmi et al., 2021b). The results of this study are inconsistent with its findings in all four building orientations. The results of this study show that overhang shading devices are more effective than overhang with side fins shading devices at 0° and 180° building orientations. The most suitable shading device for the 90° and -90° building orientation was the egg-crate shading device. However, the result of this study is that overhang shading devices are more effective than egg-crate shading devices on 0° and 180°building orientations. The egg-crate shading devices are more effective than the overhang shading devices at 90° and -90° building orientations.

Table 5 Appropriate ratio for four common types of shading devices in 16 building orientations

Orientations	Overhang Shading Devices	Side Fins Shading Devices	Overhang with Side Fins Shading Devices	Egg-crate Shading Devices
0°	0-0.5	0-0.6	0-0.4	0-0.2
22.5°	0.1-0.6	0.1-0.7	0.1-0.4	0-0.2
45°	0.2-0.6	0.3-0.6	0.2-0.5	0.1-0.3
67.5°	0.3-0.8	0.3-0.7	0.3-0.6	0.2-0.3
90°	0.4-1.0	0.3-0.9	0.4-0.7	0.2-0.4
112.5°	0.5-1.0	0.4-0.8	0.4-0.7	0.2-0.4
135°	0.5-1.0	0.4-0.9	0.4-0.9	0.3-0.4
157.5°	0.5-0.9	0.5-1.1	0.5-0.8	0.2-0.3
180°	0.5-0.9	0.5-1.2	0.4-0.8	0.2-0.3
-157.5°	0.6-1.0	0.6-1.2	0.5-0.9	0.2-0.3
-135°	0.7-1.1	0.7-1.2	0.6-0.9	0.2-0.4
-112.5°	0.7-1.2	0.7-1.1	0.6-0.9	0.3-0.4
-90°	0.7-1.2	0.8-1.1	0.6-0.9	0.3-0.5
-67.5°	0.5-0.8	0.6-0.9	0.5-0.9	0.3-0.5
-45°	0.4-0.6	0.4-0.7	0.3-0.6	0.3-0.4
-22.5°	0.3-0.6	0.4-0.8	0.3-0.7	0.2-0.3

5. Conclusions

By combining field measurements with simulation, this study identified the most suitable type of shading device for each of the 16 building orientations, as well as the appropriate ratio ranges for four common types of shading device at each orientation. The findings contribute to improving the indoor environmental performance of faculty office buildings in tropical regions, thereby reducing energy consumption. The main conclusions are as follows:

1. The faculty office in the study area exhibited poor indoor thermal performance as the compliance rate of IAT was only 72.54%.
2. The most suitable shading device for the -45° building orientation (Northwest) is the egg crate shading device. Applying it at an appropriate ratio increased compliance rate of IAT of the test room by 20.7%.
3. The building orientations for which the overhang shading device was identified as the most suitable type are 0°, 22.5°, 135°, 157.5°, 180° and -135°. The building orientations for which the overhang with side fins shading device was identified as the most suitable type are 67.5°, -157.5°, -112.5° and -22.5°. The building orientations for which the egg-crate shading device was identified as the most suitable type are 45°, 90°, 112.5°, -90°, -67.5° and -45°.

There are some limitations to this study. The findings of this study are limited to tropical region. Future research could explore the effectiveness of shading devices in other climatic regions to understand how different environmental conditions affect the performance of shading devices. The exploration of the buildings focused on faculty office, which was mid-rise building with relatively low human traffic. Future research could explore the impact of shading devices on high-traffic spaces. Understand how shading devices affect the indoor environmental performance of more densely occupied spaces.

Acknowledgements

The authors would like to express their sincere gratitude to the Faculty of Built Environment and Surveying, Universiti Teknologi Malaysia, for providing the measurement equipment and test room used in this study.

Conflicts of Interest

The author(s) declare(s) that there is no conflict of interest regarding the publication of this paper

References

Abdelwahab, S., & Sobh, H. (2022). Visual Discomfort Analysis as a Tool to Support Façade Shading Design: A Case Study in the Architectural Design Studio. *Journal of Architectural Engineering*, *28*(2): 05022003. DOI: https://doi.org/10.1061/(ASCE)AE.1943-5568.0000533

Abdul Rahim, S. N., Zakaria, M. A., Yasin, M. N., & Hanipah, M. H. (2024). Thermal comfort of student in classroom with elevated set point air-conditioner temperature: Objective and subjective measurement. *IOP Conference Series: Earth and Environmental Science*, *1347*(1): 012035. DOI: https://doi.org/10.1088/1755-1315/1347/1/012035

Abuelnuor, A. A. A., Mohammedali, A. A. M., Omara, A. A. M., Wedaa, S. A. M., Mohammed, M. O. A., Ahmed, A.-H. F. A. A.-H., & Mohamed, E.-M. E. E. (2021). Evaluation of Thermal Comfort in Academic Buildings at Khartoum Locality: A Case Study. *2020 International Conference on Computer, Control, Electrical, and Electronics Engineering (ICCCEEE)*, 1–5. DOI: https://doi.org/10.1109/ICCCEEE49695.2021.9429574

Alajmi, A., Aba-alkhail, F., & ALAnzi, A. (2021a). Determining the optimum fixed solar-shading device for minimizing the energy consumption of a side-lit office building in a scorching climate. *Journal of Engineering Research*, *9*(2): 2. DOI: https://doi.org/10.36909/jer.v9i2.10773

Alajmi, A., Aba-alkhail, F., & ALAnzi, A. (2021b). Determining the optimum fixed solar-shading device for minimizing the energy consumption of a side-lit office building in a scorching climate. *Journal of Engineering Research*, *9*(2): 2. DOI: https://doi.org/10.36909/jer.v9i2.10773

Alsukkar, M., Hu, M., Alkhater, M., & Su, Y. (2023). Daylighting performance assessment of a split louver with parametrically incremental slat angles: Effect of slat shapes and PV glass transmittance. *Solar Energy*, *264*: 112069. DOI: https://doi.org/10.1016/j.solener.2023.112069

Alwetaishi, M., Al-Khatri, H., Benjeddou, O., Shamseldin, A., Alsehli, M., Alghamdi, S., & Shrahily, R. (2021). An investigation of shading devices in a hot region: A case study in a school building. *Ain Shams Engineering Journal*, *12*(3): 3229–3239. DOI: https://doi.org/10.1016/j.asej.2021.02.008

American Society of Heating, Refrigerating and Air-Conditioning Engineers [ASHRAE]. (2013). Thermal environmental conditions for human occupancy (ANSI/ASHRAE Standard 55-2013). Atlanta, GA: Author.

Aw, S. B., Leng, P. C., & Ling, G. H. T. (2023). Facilitation of visual adaptation to glare control for daytime fire evacuation from an office building in Malaysia. *Journal of Engineering Research*. 12(2): 1-10. DOI: https://doi.org/10.1016/j.jer.2023.10.010

Baghoolizadeh, M., Rostamzadeh-Renani, M., Rostamzadeh-Renani, R., & Toghraie, D. (2023). Multi-objective optimization of Venetian blinds in office buildings to reduce electricity consumption and improve visual and thermal comfort by NSGA-II. *Energy and Buildings*, *278*: 112639. DOI: https://doi.org/10.1016/j.enbuild.2022.112639

C, C., Sasidhar, K., & Madhumathi, A. (2023). Energy-efficient retrofitting with exterior shading device in hot and humid climate – case studies from fully glazed multi-storied office buildings in Chennai, India. *Journal of Asian Architecture and Building Engineering*, *22*(4): 2209–2223. DOI: https://doi.org/10.1080/13467581.2022.2145208

Chai, K., Yu, J., Tian, Y., Zhao, A., Gao, J., & Nie, J. (2020). Comprehensive Evaluation Method of Office Building Energy Consumption Based on Improved Multi-index. *IOP Conference Series: Materials Science and Engineering*, *790*(1): 012047. DOI: https://doi.org/10.1088/1757-899X/790/1/012047

Dev, G., & Saifudeen, A. (2023). Dynamic facade control systems for optimal daylighting, a case of Kerala. *Sustainability Analytics and Modeling*, *3*: 100018. DOI: https://doi.org/10.1016/j.samod.2023.100018

Do, C. T., & Chan, Y.-C. (2021). Daylighting performance analysis of a facade combining daylight-redirecting window film and automated roller shade. *Building and Environment*, *191*: 107596. DOI: https://doi.org/10.1016/j.buildenv.2021.107596

Eltaweel, A., Su, Y., Mandour, M. A., & Elrawy, O. O. (2021). A novel automated louver with parametrically-angled reflective slats; design evaluation for better practicality and daylighting uniformity. *Journal of Building Engineering*, *42*: 102438. DOI: https://doi.org/10.1016/j.jobe.2021.102438

Gamero-Salinas, J. C., Monge-Barrio, A., & Sánchez-Ostiz, A. (2020). Overheating risk assessment of different dwellings during the hottest season of a warm tropical climate. *Building and Environment*, *171*: 106664. DOI: https://doi.org/10.1016/j.buildenv.2020.106664

Huo, H., Xu, W., Li, A., Cui, G., Wu, Y., & Liu, C. (2020). Field comparison test study of external shading effect on thermal-optical performance of ultralow-energy buildings in cold regions of China. *Building and Environment*, *180*: 106926. DOI: https://doi.org/10.1016/j.buildenv.2020.106926

Koç, S. G., & Maçka Kalfa, S. (2021). The effects of shading devices on office building energy performance in Mediterranean climate regions. *Journal of Building Engineering*, *44*: 102653. DOI: https://doi.org/10.1016/j.jobe.2021.102653

Kunwar, N., Cetin, K. S., & Passe, U. (2021). Calibration of energy simulation using optimization for buildings with dynamic shading systems. *Energy and Buildings*, *236*: 110787. DOI: https://doi.org/10.1016/j.enbuild.2021.110787

Lau, A. K. K., Salleh, E., Lim, C. H., & Sulaiman, M. Y. (2016). Potential of shading devices and glazing configurations on cooling energy savings for high-rise office buildings in hot-humid climates: The case of Malaysia. *International Journal of Sustainable Built Environment*, *5*(2): 387–399. DOI: https://doi.org/10.1016/j.ijsbe.2016.04.004

Mangkuto, R. A., Koerniawan, M. D., Apriliyanthi, S. R., Lubis, I. H., Atthaillah, Hensen, J. L. M., & Paramita, B. (2022). Design Optimisation of Fixed and Adaptive Shading Devices on Four Façade Orientations of a High-Rise Office Building in the Tropics. *Buildings*, *12*(1): Article 1. DOI: https://doi.org/10.3390/buildings12010025

Mohammed, A., Tariq, M. A. U. R., Ng, A. W. M., Zaheer, Z., Sadeq, S., Mohammed, M., & Mehdizadeh-Rad, H. (2022). Reducing the Cooling Loads of Buildings Using Shading Devices: A Case Study in Darwin. *Sustainability*, *14*(7): Article 7. DOI: https://doi.org/10.3390/su14073775

Mustapa, M. S., Zaki, S. A., Rijal, H. B., Hagishima, A., & Ali, M. S. M. (2016). Thermal comfort and occupant adaptive behaviour in Japanese university buildings with free running and cooling mode offices during summer. *Building and Environment*, *105*: 332–342. DOI: https://doi.org/10.1016/j.buildenv.2016.06.014

Oleiwi, M. Q., & Mohamed, M. F. (2022). The Impacts of Passive Design Strategies on Building Indoor Temperature in Tropical Climate. *Pertanika Journal of Science and Technology*, *31*(1): 83–108. DOI: https://doi.org/10.47836/pjst.31.1.06

Rana, Md. J., Hasan, Md. R., & Sobuz, Md. H. R. (2021). An investigation on the impact of shading devices on energy consumption of commercial buildings in the contexts of subtropical climate. *Smart and Sustainable Built Environment*, *11*(3): 661–691. DOI: https://doi.org/10.1108/SASBE-09-2020-0131

Rana, Md. J., Hasan, Md. R., & Sobuz, Md. H. R. (2022a). An investigation on the impact of shading devices on energy consumption of commercial buildings in the contexts of subtropical climate. *Smart and Sustainable Built Environment*, *11*(3): 661–691. DOI: https://doi.org/10.1108/sasbe-09-2020-0131

Rana, Md. J., Hasan, Md. R., & Sobuz, Md. H. R. (2022b). An investigation on the impact of shading devices on energy consumption of commercial buildings in the contexts of subtropical climate. *Smart and Sustainable Built Environment*, *11*(3): 661–691. DOI: https://doi.org/10.1108/SASBE-09-2020-0131

Rijal, H. B., Humphreys, M. A., & Nicol, J. F. (2017). Towards an adaptive model for thermal comfort in Japanese offices. *Building Research & Information*, *45*(7): 717–729. DOI: https://doi.org/10.1080/09613218.2017.1288450

Settino, J., Carpino, C., Perrella, S., & Arcuri, N. (2020). Multi-Objective Analysis of a Fixed Solar Shading System in Different Climatic Areas. *Energies*, *13*(12): Article 12. DOI: https://doi.org/10.3390/en13123249

Shaaban, A. K., Khudhayer, W. A., & Sukor, N. S. A. (2017). Total shading system approach at Sultan Qaboos University Eco-House project. *AIP Conference Proceedings*, *1892*(1): 160011. DOI: https://doi.org/10.1063/1.5005778

Su, M. A., Ngarambe, J., Santamouris, M., & Yun, G. Y. (2021). Empirical evidence on the impact of urban overheating on building cooling and heating energy consumption. *iScience*, *24*(5): 102495. DOI: https://doi.org/10.1016/j.isci.2021.102495

Tayag, C. R. C., & Conejos, S. (2025). Passive cooling in tropical residential buildings using thermal and energy performance analysis. *IOP Conference Series: Earth and Environmental Science*, *1500*(1): 012060. DOI: https://doi.org/10.1088/1755-1315/1500/1/012060

Tong, S., Wen, J., Wong, N. H., & Tan, E. (2021). Impact of façade design on indoor air temperatures and cooling loads in residential buildings in the tropical climate. *Energy and Buildings*, *243*: 110972. DOI: https://doi.org/10.1016/j.enbuild.2021.110972

Valitabar, M., GhaffarianHoseini, Ali, GhaffarianHoseini, Amirhosein, & Attia, S. (2022). Advanced control strategy to maximize view and control discomforting glare: A complex adaptive façade. *Architectural Engineering and Design Management*, *18*(6): 829–849. DOI: https://doi.org/10.1080/17452007.2022.2032576

Wang, Y., Yang, W., & Wang, Q. (2022). Multi-objective parametric optimization of the composite external shading for the classroom based on lighting, energy consumption, and visual comfort. *Energy and Buildings*, *275*: 112441. DOI: https://doi.org/10.1016/j.enbuild.2022.112441

Yao, B., Salehi, A., Baghoolizadeh, M., Khairy, Y., & Baghaei, Sh. (2024). Multi-objective optimization of office egg shadings using NSGA-II to save energy consumption and enhance thermal and visual comfort. *International Communications in Heat and Mass Transfer*, *157*: 107697. DOI: https://doi.org/10.1016/j.icheatmasstransfer.2024.107697

Zheng, Y., Wu, J., Zhang, H., Lin, C., Li, Y., Cui, X., & Shen, P. (2025). A novel sun-shading design for indoor visual comfort and energy saving in typical office space in Shenzhen. *Energy and Buildings*, *328*: 115083. DOI: https://doi.org/10.1016/j.enbuild.2024.115083